This is an open access article published under a Creative Commons Attribution (CC-BY) License, which permits unrestricted use, distribution and reproduction in any medium, provided the author and source are cited.

Biochemistry

Article

Cite This: Biochemistry 2018, 57, 6228−6233

pubs.acs.org/biochemistry

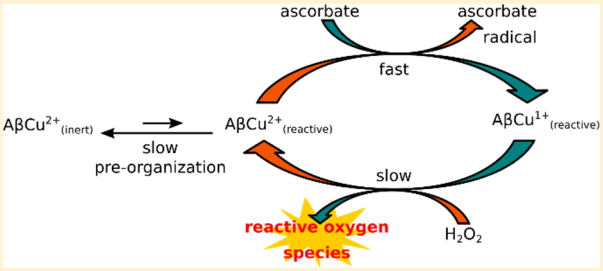
Redox Kinetics of the Amyloid-β-Cu Complex and Its Biological Implications

Paul Girvan,[†,§] Xiangyu Teng,[†] Nicholas J. Brooks,[†,§] Geoffrey S. Baldwin,[*,§,‡] and Liming Ying[*,§,#]

[†]Department of Chemistry, [§]Institute of Chemical Biology, [‡]Department of Life Sciences and [#]National Heart and Lung Institute, Imperial College London, London SW7 2AZ, United Kingdom

Supporting Information

ABSTRACT: The ability of the amyloid-β peptide to bind to redox active metals and act as a source of radical damage in Alzheimer's disease has been largely accepted as contributing to the disease's pathogenesis. However, a kinetic understanding of the molecular mechanism, which underpins this radical generation, has yet to be reported. Here we use a sensitive fluorescence approach, which reports on the oxidation state of the metal bound to the amyloid-β peptide and can therefore shed light on the redox kinetics. We confirm that the redox goes via a low populated, reactive intermediate and that the reaction proceeds via the Component **I** coordination environment rather than Component **II**. We also show that while the reduction step readily occurs (on the 10 ms time scale) it is the oxidation step that is rate-limiting for redox cycling.



Downloaded via IMPERIAL COLLEGE LONDON on November 29, 2018 at 14:58:55 (UTC).
See https://pubs.acs.org/sharingguidelines for options on how to legitimately share published articles.

Dyshomeostasis of metal ions is often implicated in the development of Alzheimer's disease (AD).[1,2] It is most often mentioned regarding the ability of metals to impact upon the aggregation of amyloid-β (Aβ), a central tenet of the amyloid cascade hypothesis, which states that aggregation and deposition of amyloid-β peptides are the central event in Alzheimer's disease.[3−5] Indeed these Aβ plaques (the hallmark of AD) are highly enriched with metal ions, suggesting a link between Aβ and metal ions.[6] Another observation about these plaques is that Aβ is found in an oxidized form, and generally, a large amount of oxidative damage (to proteins, lipids, and nucleic acids) is observed in the AD brain.[7−9] This links the second area where metal ions are implicated in AD; metal ion redox cycling is a source of reactive oxygen species (ROS) and thus can lead to oxidative damage within the AD brain.[10,11]

While these Aβ plaques are found with a multitude of different metals, the majority of research is directed toward the study of the Aβ-Cu complex. Many in vitro studies have shown that in the presence of a reducing agent (e.g., ascorbate) the Aβ-Cu complex can generate ROS ($O_2^{-\bullet}$, H_2O_2, $OH^\bullet$).[12] Indeed, the similarities between the redox cycling of the Aβ-Cu complex and that of the metal ions at the center of the Fenton and Haber−Weiss mechanisms have not gone unnoticed.[13,14] Because the Aβ-Cu complex is potentially a source of ROS in AD, a great effort has been directed toward understanding the interaction between Aβ and Cu.

For the Aβ-Cu(II) complex, EPR studies have revealed that the Aβ peptide coordinates to the Cu(II) center with a square planar geometry involving a combination of the first two amino acids and up to two histidine ligands (Figure 1A). Additionally, due to the flexible nature of this intrinsically disordered peptide, there is not one single well-defined binding pocket in which Cu(II) sits. Instead two major populations of Aβ-Cu(II) complex coexist at a physiological pH, differing in their protonation state and coordinating amino acids.[15] These two coordination environments (referred to as Component **I** and Component **II** for the protonated and deprotonated species, respectively) were found to be in dynamic equilibrium with each other, interconverting on the second time scale (Figure 1A).[16] It is also reported that Aβ can bind Cu(II) at near diffusion limited kinetics, with a modestly low nM K_d under physiological conditions and that, in the synapse (where concentrations of Cu transiently reach high enough concentrations), the Aβ peptide can kinetically compete for Cu,

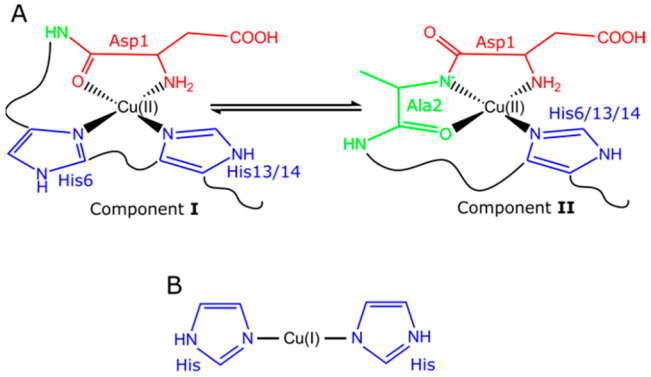


Figure 1. (A) Square planar coordination environments for the two major species of the Cu(II) complex (Components **I** and **II**). (B) Linear coordination of the Aβ-Cu(I) complex.

Received: February 3, 2018
Revised: September 25, 2018
Published: September 28, 2018

© 2018 American Chemical Society

DOI: 10.1021/acs.biochem.8b00133
Biochemistry 2018, 57, 6228−6233

suggesting that the Aβ-Cu(II) complex can transiently exist in certain locations within the brain.[16−18] By comparison, the Aβ-Cu(I) species displays a linear geometry involving two out of the three possible histidine residues (Figure 1B) and has been shown to have a similar K_d to the Aβ-Cu(II) species.[19,20]

As it is the redox cycling of the Aβ-Cu complex that is implicated in the progression of AD, the mechanism and kinetics of the reduction and oxidation steps are of particular interest. Due to the differences between the major Cu(I/II) species coordinating environments, direct electron transfer between them requires a significant ligand rearrangement. Electrochemical studies have demonstrated that this is unfeasible and instead proposed that the redox went via a "catalytic in between state" (CIBS), where the ligands are better arranged to facilitate fast redox cycling.[21] This reactive CIBS was suggested to make up a small fraction of the Aβ-Cu complex and is hard to directly observe with EPR. Nevertheless, efforts were directed toward identifying the residues most likely involved in the coordination of this reactive intermediate. Techniques including HPLC/MS, fluorescence, and UV−vis were utilized in the determination of the CIBS structure, leading to the proposal of a potential redox mechanism.[22,23]

Previously we have reported the use of a fluorescence-based kinetic approach for studying the interactions of Aβ and Cu, which is highly sensitive to the copper environment.[16] Now we describe the use of our kinetic approach to verify the presence of the low-populated, reactive intermediate state via a completely orthogonal technique. Finally, we aim to quantify the kinetics of the redox system to address whether Aβ-Cu redox occurs on a biologically relevant time scale, therefore being relevant to the progression of AD, an issue which has currently received little attention.

In order to study the redox kinetics of the amyloid-β copper complex, we utilized a truncated Aβ peptide that was fluorescently labeled at the C-terminus. This truncated Aβ, consisting of the first 16 residues, is often employed as the model system of choice when studying Aβ metal interactions, as it contains the metal binding residues without displaying peptide aggregation.

Upon binding of Cu(II), the fluorescently labeled Aβ peptide is quenched, due to the fluorophore being in close proximity with the paramagnetic Cu(II) ion. As the quenching is due to the paramagnetic nature of the Cu(II) ion having one single unpaired electron, when this copper center is reduced to the +1 oxidation state, it becomes diamagnetic and no longer quenches the nearby C-terminal fluorophore. We should therefore observe a recovery of fluorescence upon reduction of Aβ-Cu(II) to Aβ-Cu(I) and as such have a system able to report on the oxidation state of the copper center in the Aβ-Cu complex with a fluorescent readout.

MATERIALS AND METHODS

Materials. The amyloid-β peptides used in this work were all obtained labeled with HiLyte Fluor 488. For Aβ16 (which is used throughout this work unless explicitly stated otherwise), the fluorophore was placed on the C-terminal lysine residue. For Aβ40, the fluorophore was introduced at position 20, which was mutated to cysteine. All peptides were bought from or custom synthesized by AnaSpec via Cambridge Bioscience. The concentration of stock solutions of the fluorescently labeled Aβ peptides were determined using the dye peak absorbance and an extinction coefficient of ε = 68 000 cm^{-1} M^{-1}.

Steady-state fluorescent measurements were made using a FluoroMax-4 (HORIBA) fluorometer. The fluorescently labeled Aβ peptide was excited at 488 nm, while emission was recorded at 525 nm. For each point, three measurements were taken, and the mean and standard deviation were reported. Excitation and emission slit widths were chosen such that the fluorescent intensity was ca. 10^4−10^5 counts per second to remain well within the linear range of the instrument. Integration time for each point was set to 1 s.

Stopped-flow measurements were made using a KinetAsyst SF-61DX2 stopped-flow spectrophotometer (HI-TECH Scientific). Excitation was provided using a fiber coupled diode laser (MCLS1-473-20, Thorlabs) at 473 nm. Fluorescence emission was filtered using a 515 nm long pass filter (515GY, Comar) before detection by a photomultiplier tube. For each data point, a minimum of 7 traces were averaged. Raw data was fit using OriginPro 2015 (OriginLab) using the sum of two exponential functions.

For the single-mixing reduction kinetics, one syringe containing Aβ-Cu(II) was rapidly mixed with a second syringe containing variable concentrations of ascorbate. The final concentrations after mixing were 50 nM Aβ-Cu(II), and the ascorbate concentrations were given in the figure captions.

For double-mixing reduction kinetics, Aβ in one syringe was rapidly mixed with Cu(II) in a second syringe. After this first mixing, the concentrations were 50 nM Aβ and 1 μM Cu(II). This mixture was allowed to react for between 100 ms and 5 s. Following this delay, this mixture was then mixed with a third syringe containing ascorbate, giving a final concentration of ascorbate of 1 mM.

For double-mixing oxidation kinetics, Aβ-Cu(II) in one syringe was rapidly mixed with ascorbate in a second syringe, giving final concentrations of 100 nM Aβ-Cu(II) and 50 μM ascorbate. The reaction was allowed to proceed for 5 s before this initial mixture was mixed with H_2O_2 in a variety of concentrations.

More detailed methodology and materials are provided in the Supporting Information.

RESULTS AND DISCUSSION

To investigate the reduction of the Aβ-Cu(II) and confirm that recovery of fluorescence upon reduction to Aβ-Cu(I) is observable, a fluorescence titration experiment was performed (Figure 2). When a high enough concentration of ascorbate (Asc) is added to the Aβ-Cu(II) complex, an increased fluorescence is observed, consistent with the metal center going from the +2 to the +1 oxidation state. Fitting the curve with a Hill function reveals that 1.4(1) μM ascorbate is required for half recovery of fluorescence.

To study the kinetics of the reduction process, the complex was preformed before mixing with various concentrations of ascorbate while fluorescence recovery was recorded as a function of time using a stopped-flow apparatus (Figure 3A). It can be seen that the rate of rise in fluorescence increases as the ascorbate concentration gets higher, as is expected for a reaction involving at least two species. In addition, at high concentrations of ascorbate, two phases begin to become apparent within the traces. The faster phase increases with higher concentrations of ascorbate, while the slower phase has no dependence on the ascorbate concentration. This is more clearly illustrated in Figure 3B, which shows the fitting

DOI: 10.1021/acs.biochem.8b00133
Biochemistry 2018, 57, 6228−6233

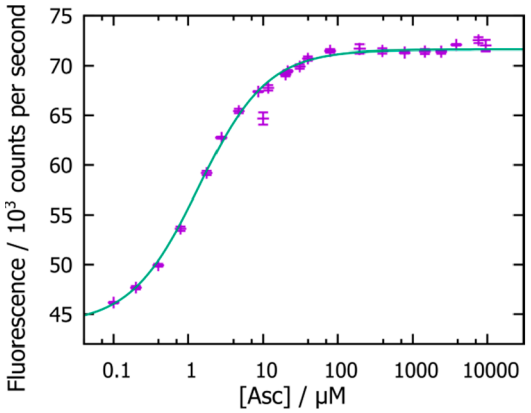


Figure 2. Titration of ascorbate into 1 μM Aβ-Cu(II) in N_2 purged HEPES buffer. Error bars show the standard deviation of three measurements. Fluorescence intensity was corrected for collisional quenching induced by high ascorbate (Figure S1).

parameters from a double exponential fit of the raw fluorescent traces while varying ascorbate concentration over a 3-order magnitude range. The same biphasic response was observed for the Aβ40-Cu(II) complex though the reaction rate is slightly different (Figure S2).

It has been suggested that redox, and ultimately ROS generation, is via the Component **I** Aβ-Cu(II) coordination (Figure 1A); however, kinetic data supporting this has not yet been presented. We addressed this question using double-mixing stopped-flow. By rapidly mixing Aβ and Cu(II) and then, after various delay times, mixing with ascorbate, we can probe the reactivity of each component as the relative populations evolve temporally. If Component **I** forms first and is the most reactive, we would predict that at very short delay times (i.e., before the system has had time to interconvert to Component **II**) we would observe the fastest reaction. Conversely, at long delay times, when the system has reached equilibrium and the relative population of Component **II** has increased, we would observe a slower reduction upon mixing with ascorbate. This is indeed what we observe (Figure 3C). It can also be noted that the amplitudes of the fast and slow phases change as a function of delay time. At short delay times, when Component **I** dominates the system, the amplitude of the fast phase is greater than the amplitude of the slow phase, while at longer delay times when the proportion of Component **II** has increased, the amplitude of the slow phase likewise increases. This is more easily visualized in Figure 3D, which shows how the relative amplitudes evolve as a function of delay time.

To confirm our assignment of the fast and slow phases to Components **I** and **II**, respectively, we have also studied the reduction of the human Aβ containing an A2P mutation (A2P-Aβ) and the murine Aβ peptide (mAβ) (Figure S3). The introduction of these mutations (mAβ differs from the human peptide at three positions, R5G, Y10F, H13R) slightly alters the Cu(II) coordination environments. These altered coordination environments affect the relative proportions of Components **I** and **II**.[24,25] While human Aβ has a pK_a for Component **I**↔**II** of 7.7, mAβ is much lower at 6.2 and A2P-Aβ is much higher at 8.8.[24,25] Therefore, under our

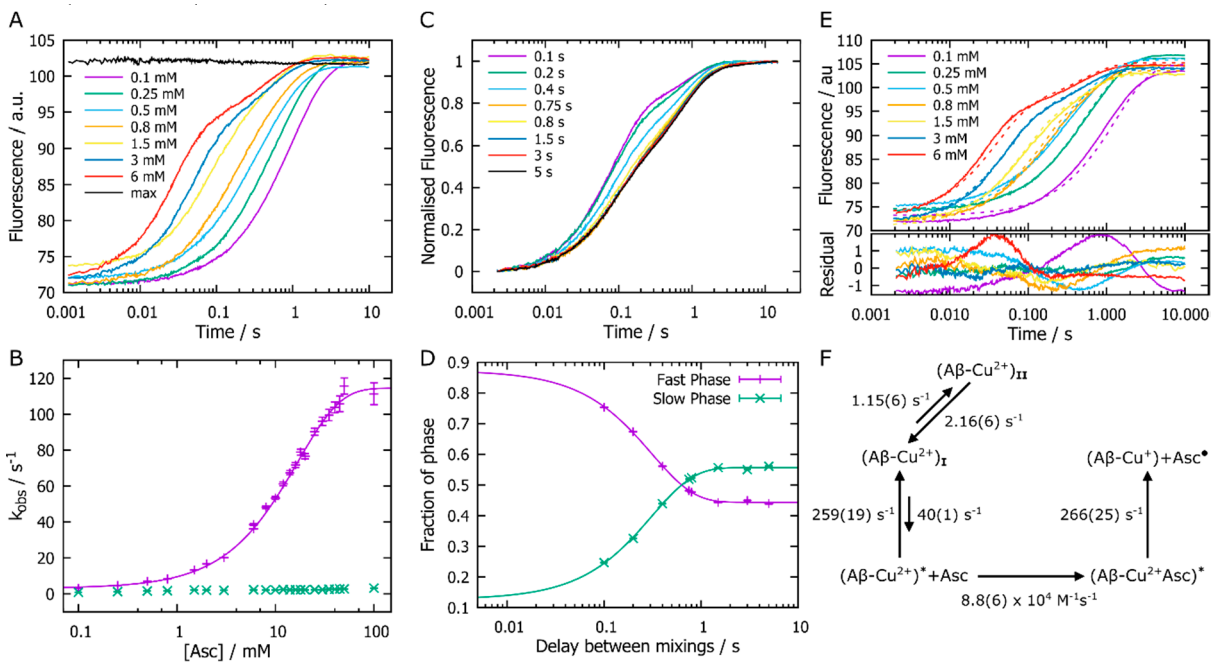


Figure 3. Reduction kinetics of Aβ-Cu(II). (A) Stopped-flow kinetic traces showing the recovery of fluorescence after mixing 50 nM Aβ-Cu(II) with ascorbate (concentration in key), max signal from 50 nM Aβ (no Cu(II) or ascorbate) showing that reduction of Aβ-Cu(II) gives full recovery of fluorescence. (B) Rate of fast and slow phases against ascorbate concentration. Rates determined from fitting data in panel A to a double exponential. Rates determined for the fast phase are shown fitted to a single exponential. (C) Kinetics of reduction probed by double-mixing stopped-flow. Aβ (100 nM) was first mixed with 2 μM Cu(II) (1:1 volume) and then after a variable delay (see key) with 2 mM ascorbate (1:1 volume). (D) Temporal evolutions of the fractions of the two phases. (E) Stopped-flow traces showing the reduction of Aβ-Cu(II) by ascorbate; dashed lines show the expected traces given the mechanism and rate constants shown in panel F. All experiments were performed at pH 7.5 and at a temperature of 298 K. Each fluorescent trace (top panels) is the average of at least seven repeat measurements. Error bars are the uncertainty of the fit.

DOI: 10.1021/acs.biochem.8b00133
Biochemistry 2018, 57, 6228−6233

experimental pH of 7.5, human Aβ would have two components coexisting, while for the two controls only either Component **I** or Component **II** would predominate. Indeed, as shown in Figure S3, only one phase was dominant for both mAβ and A2P-Aβ. For A2P-Aβ, the kinetics matches the fast phase of human Aβ, while for mAβ, the kinetics matches the slow phase of human Aβ.

This data provides evidence that the reduction step of the redox cycling of the Aβ-Cu(II) complex proceeds via the Component **I** coordination and that reduction of Component **II** either does not occur, or occurs slower than interconversion to Component **I** and subsequent reduction. While these data suggest that the reduction step of redox cycling occurs via Component **I**, it does not provide evidence that Component **I** is the species that directly undergoes reduction. Indeed, by observing which residues on the Aβ peptide are most frequently damaged by redox cycling, Cassagnes et al. have suggested that Aβ-Cu(II) is not directly reduced to the Aβ-Cu(I) complex, but rearranges its coordination sphere to a low-populated, highly reactive intermediate, which is amenable to fast electron transfer.[22] This is consistent with electrochemical data noting that the energy to go directly between Aβ-Cu(II) and Aβ-Cu(I) is too high to be biologically attainable.[21]

In the coordination environment of this highly reactive intermediate, it was noted that the copper was bound by Asp1 and either His13 or His14 but crucially that His6 (which forms part of the Component **I** coordination) was not coordinating to the copper center.[22,23] One may argue that if His6 is not involved in the reduction step, a mutation at this residue should not affect the kinetics of reduction. To test this, we used the Familial Alzheimer's disease relevant H6R-Aβ mutant peptide, which is one of several mutations that causes early onset Alzheimer's disease.[26] It has been shown that the H6R-Aβ mutation does not affect the production of Aβ and is also able to bind copper with similar kinetics to the wild-type; however, H6R-Aβ displays a greater propensity toward aggregation.[27−29]

For the reduction kinetics of the H6R-Aβ peptide, we found that they were indistinguishable from the wild-type Aβ (Figure S4). As such, our kinetic data provides further weight to the proposed coordination of the highly reactive intermediate not involving His6.

To further probe the validity of this low-populated reactive intermediate state, we attempted to see if our experimental data could be fit to such a mechanism.[22] Figure 3F shows a modified version of this mechanism, which was fit to our data using KinTek Explorer.[30] Figure 3E shows that a good fit of the data to the model can be achieved. The fitted rate constants for the conversion from the main Component **I** conformation of Aβ-Cu(II) to the intermediate capable of fast redox show that the equilibrium lies heavily on the side of Component **I**. Reassuringly, the rate constants determined from the fit for the interconversion between Component **I** and **II** species are within error of values previously reported.[16] Overall, the rate constants determined suggest that the reduction step happens on the ms time scale, with the conformational selection step of the mechanism being the rate-limiting step.

For the oxidation side of the redox cycle, the experiments are much less tractable. Cu(I) salts are unstable in air or solution, either reacting with oxygen or undergoing disproportionation to give Cu(0) and Cu(II). To circumvent these problems, we used a double-mixing stopped-flow approach whereby Aβ-Cu(II) was first reduced by ascorbate to generate Aβ-Cu(I) in situ and then, after a short delay, oxidized back to Aβ-Cu(II) with hydrogen peroxide. Under these experimental conditions, there will be both ascorbate and hydrogen peroxide present after the final mixing step. Therefore, as the reaction progresses, both oxidation and reduction of Aβ-Cu will be taking place. By limiting the data analysis to the initial portion of the kinetic trace, we can extract the initial rate by approximation with a straight line. At these early time points, the concentration of Aβ-Cu(II) will be effectively zero (i.e., no reduction will be able to take place), and we will be observing just the oxidation process. Figure 4 shows how the initial rate

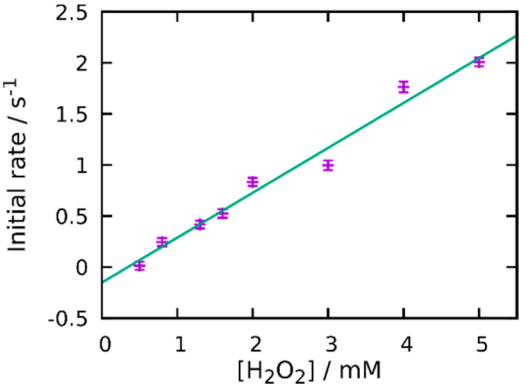


Figure 4. Initial rate of Aβ-Cu(I) oxidation against H_2O_2 concentration. Aβ-Cu(II) was reduced with ascorbate before being reoxidized by various concentrations of H_2O_2. Experiment was performed at 298 K and at pH 7.5. The error bars show the standard deviation of the fit.

of oxidation of Aβ-Cu(I) varies with H_2O_2 concentration. The rate of oxidation varies linearly with an increasing H_2O_2 concentration, indicating a bimolecular association process, with an apparent second-order rate constant of $4.4(2) \times 10^2$ M^{-1} s^{-1}. This oxidation rate constant is independent of the ascorbate concentration used to generate the Aβ-Cu(I) (Figure S5).

Our kinetic result suggests that the oxidation step is the limiting factor in redox cycling of the Aβ-Cu complex and ultimately ROS generation; however, it should be noted that the reduction step alone is capable of generating radical species and initiating radical chain reactions.

CONCLUSIONS

If ROS damage generated from the amyloid-β metal complex is involved in the pathogenesis of Alzheimer's disease, we must understand the reduction and oxidation steps involved. To this end, we have measured the kinetics of Aβ-Cu reduction and oxidation by observing the change in oxidation state of the coordinated metal ion. We have developed a method that directly reports on the oxidation state of the metal ion in the Aβ complex. This enabled single turnover kinetics to be measured, allowing us to link a detailed mechanistic insight into proposed binding modalities of the Aβ-Cu complex.

We found that oxidation is the limiting step in redox cycling of the Aβ-Cu complex. For the reduction half, we have shown that it is indeed Component **I** that preferentially undergoes reduction, while Component **II** does not.

The kinetic data displayed in this study is consistent with a conformational selection mechanism,[31] whereby the main Aβ-

DOI: 10.1021/acs.biochem.8b00133
Biochemistry 2018, 57, 6228−6233

Cu(II) Component **I** complex must first convert to a low-populated species where the coordinating amino acids are arranged more favorably for redox to occur, in agreement with literature.[22,23] The fitted rate constants show that the equilibrium does lie heavily away from the reactive intermediate and that the reduction step itself happens fairly rapidly, on the millisecond time scale. Whereas the whole brain ascorbate concentration is 1 to 2 mM, intracellular neuronal concentrations are much higher.[32] Therefore, the binding of ascorbate to the Aβ-Cu complex is not rate-limiting in the reduction mechanism, while the preorganization of the complex to the minor intermediate state is. Overall, the reduction would occur on the 10 ms time scale, much faster than the lifetime of the Component **I** complex (dissociation rate constant ca. 0.8 s^{-1}).[16] The oxidation is expected to be much slower since the physiological H_2O_2 concentration within the brain is reported in the μM regime.[33,34] Taken together, this data suggests that while the reduction step is highly capable of generating damaging radicals, the oxidation step will occur less frequently. Nevertheless, the reduction and oxidation of the Aβ-Cu complex occur on physiologically relevant time scales. As such, these processes may contribute to the oxidative damage observed in Alzheimer's disease.

■ ASSOCIATED CONTENT

Supporting Information

The Supporting Information is available free of charge on the ACS Publications website at DOI: 10.1021/acs.biochem.8b00133.

Experimental materials, fluorometer measurements, Stern–Volmer plot, reduction kinetics, stopped-flow data, assignment of the fast and slow phases of reduction, and oxidation control experiments (PDF)

■ AUTHOR INFORMATION

Corresponding Authors

*E-mail: g.baldwin@imperial.ac.uk.
*E-mail: l.ying@imperial.ac.uk.

ORCID

Nicholas J. Brooks: 0000-0002-1346-9559
Liming Ying: 0000-0001-9752-6292

Author Contributions

The manuscript was written through contributions of all authors.

Funding

This work was supported by a Ph.D. studentship from the Engineering and Physical Sciences Research Council (EPSRC) of the U.K. awarded to P.G. and grants from the Leverhulme Trust (RPG-2015-345) and British Heart Foundation PG/11/81/29130.

Notes

The authors declare no competing financial interest.

■ ABBREVIATIONS

AD, Alzheimer's disease; Aβ, amyloid-beta; ROS, reactive oxygen species; Asc, ascorbate; mAβ, murine amyloid-beta.

■ REFERENCES

(1) Bush, A. I. (2003) The metallobiology of Alzheimer's disease. *Trends Neurosci. 26*, 207–214.
(2) Maynard, C. J., Bush, A. I., Masters, C. L., Cappai, R., and Li, Q. X. (2005) Metals and amyloid-β in Alzheimer's disease. *Int. J. Exp. Pathol. 86*, 147–159.
(3) Bush, A. I., Pettingell, W. H., Multhaup, G., Paradis, M. d., Vonsattel, J. P., Gusella, J. F., Beyreuther, C. L., Tanzi, R. E., and Masters, C. (1994) Rapid induction of Alzheimer A beta amyloid formation by zinc. *Science 265*, 1464–1467.
(4) Chen, W. T., Liao, Y. H., Yu, H. M., Cheng, I. H., and Chen, Y. R. (2011) Distinct Effects of Zn^{2+}, Cu^{2+}, Fe^{3+}, and Al^{3+} on Amyloid-β Stability, Oligomerization, and Aggregation. *J. Biol. Chem. 286*, 9646–9656.
(5) Tiiman, A., Palumaa, P., and Tõugu, V. (2013) The missing link in the amyloid cascade of Alzheimer's disease–metal ions. *Neurochem. Int. 62*, 367–378.
(6) Lovell, M. A., Robertson, J. D., Teesdale, W. J., Campbell, J. L., and Markesbery, W. R. (1998) Copper, iron and zinc in Alzheimer's disease senile plaques. *J. Neurol. Sci. 158*, 47–52.
(7) Smith, C. D., Carney, J. M., Starke-Reed, P. E., Oliver, C. N., Stadtman, E. R., Floyd, R. A., and Markesbery, W. R. (1991) Excess brain protein oxidation and enzyme dysfunction in normal aging and in Alzheimer disease. *Proc. Natl. Acad. Sci. U. S. A. 88* (23), 10540–10543.
(8) Butterfield, D. A., Drake, J., Pocernich, C., and Castegna, A. (2001) Evidence of oxidative damage in Alzheimer's disease brain: central role for amyloid β-peptide. *Trends Mol. Med. 7*, 548–554.
(9) Wang, J., Markesbery, W. R., and Lovell, M. A. (2006) Increased oxidative damage in nuclear and mitochondrial DNA in mild cognitive impairment. *J. Neurochem. 96*, 825–832.
(10) Cheignon, C., Tomas, M., Bonnefont-Rousselot, D., Faller, P., Hureau, C., and Collin, F. (2018) Oxidative stress and the amyloid beta peptide in Alzheimer's disease. *Redox Biol. 14*, 450–464.
(11) Markesbery, W. R. (1997) Oxidative stress hypothesis in Alzheimer's disease. *Free Radical Biol. Med. 23*, 134–147.
(12) Opazo, C., Huang, X., Cherny, R. A., Moir, R. D., Roher, A. E., White, A. R., Cappai, R., Masters, C. L., Tanzi, R. R., Inestrosa, N. C., and Bush, A. I. (2002) Metalloenzyme-like activity of Alzheimer's disease β-amyloid Cu-dependent catalytic conversion of dopamine, cholesterol, and biological reducing agents to neurotoxic H_2O_2. *J. Biol. Chem. 277* (43), 40302–40308.
(13) Smith, D. G., Cappai, R., and Barnham, K. J. (2007) The redox chemistry of the Alzheimer's disease amyloid β peptide. *Biochim. Biophys. Acta, Biomembr. 1768* (8), 1976–1990.
(14) Huang, X., Atwood, C. S., Hartshorn, M. A., Multhaup, G., Goldstein, L. E., Scarpa, R. C., Cuajungco, M. P., Gray, D. N., Lim, J., Moir, R. D., Tanzi, R. E., and Bush, A. I. (1999) The Aβ Peptide of Alzheimer's Disease Directly Produces Hydrogen Peroxide through Metal Ion Reduction. *Biochemistry 38* (24), 7609–7616.
(15) Dorlet, P., Gambarelli, S., Faller, P., and Hureau, C. (2009) Pulse EPR Spectroscopy Reveals the Coordination Sphere of Copper (II) Ions in the 1–16 Amyloid-β Peptide: A Key Role of the First Two N-Terminus Residues. *Angew. Chem. 121*, 9437–9440.
(16) Branch, T., Girvan, P., Barahona, M., and Ying, L. (2015) Introduction of a Fluorescent Probe to Amyloid-β to Reveal Kinetic Insights into Its Interactions with Copper (II). *Angew. Chem., Int. Ed. 54*, 1227–1230.
(17) Conte-Daban, A., Borghesani, V., Sayen, S., Guillon, E., Journaux, Y., Gontard, G., Lisnard, L., and Hureau, C. (2017) Link between affinity and Cu(II) binding sites to amyloid-β peptides evaluated by a new water-soluble ratiometric dye with a moderate Cu(II) affinity. *Anal. Chem. 89*, 2155–2162.
(18) Branch, T., Barahona, M., Dodson, C. A., and Ying, L. (2017) Kinetic Analysis Reveals the Identity of Aβ-Metal Complex Responsible for the Initial Aggregation of Aβ in the Synapse. *ACS Chem. Neurosci. 8*, 1970–1979.
(19) Shearer, J., and Szalai, V. A. (2008) The amyloid-β peptide of Alzheimer's disease binds CuI in a linear bis-his coordination environment: Insight into a possible neuroprotective mechanism for the amyloid-β peptide. *J. Am. Chem. Soc. 130*, 17826–17835.

DOI: 10.1021/acs.biochem.8b00133
Biochemistry 2018, 57, 6228–6233

(20) Young, T. R., Kirchner, A., Wedd, A. G., and Xiao, Z. (2014) An integrated study of the affinities of the Aβ16 peptide for Cu (I) and Cu (II): implications for the catalytic production of reactive oxygen species. *Metallomics 6* (3), 505−517.
(21) Balland, V., Hureau, C., and Savéant, J. M. (2010) Electrochemical and homogeneous electron transfers to the Alzheimer amyloid-β copper complex follow a preorganization mechanism. *Proc. Natl. Acad. Sci. U. S. A. 107*, 17113−17118.
(22) Cassagnes, L. E., Hervé, V., Nepveu, F., Hureau, C., Faller, P., and Collin, F. (2013) The Catalytically Active Copper-Amyloid-Beta State: Coordination Site Responsible for Reactive Oxygen Species Production. *Angew. Chem., Int. Ed. 52*, 11110−11113.
(23) Cheignon, C., Jones, M., Atrián-Blasco, E., Kieffer, I., Faller, P., Collin, F., and Hureau, C. (2017) Identification of key structural features of the elusive Cu−Aβ complex that generates ROS in Alzheimer's disease. *Chem. Sci. 8*, 5107−5118.
(24) Eury, H., Bijani, B. C., Faller, P., and Hureau, C. (2011) Copper (II) coordination to amyloid murine versus human peptide. *Angew. Chem., Int. Ed. 50*, 901−905.
(25) Yako, N., Young, T. R., Cottam Jones, J. M., Hutton, C. A., Wedd, A. G., and Xiao, Z. (2017) Copper binding and redox chemistry of the Aβ16 peptide and its variants: insights into determinants of copper-dependent reactivity. *Metallomics 9*, 278−291.
(26) Janssen, J. C., Beck, J. A., Campbell, T. A., Dickinson, A., Fox, N. C., Harvey, R. J., Houlden, H., Rossor, M. N., and Collinge, J. (2003) Early onset familial Alzheimer's disease Mutation frequency in 31 families. *Neurology 60* (2), 235−239.
(27) Hori, Y., Hashimoto, T., Wakutani, Y., Urakami, K., Nakashima, K., Condron, M. M., Tsubuki, S., Saido, T. C., Teplow, D. B., and Iwatsubo, T. (2007) The Tottori (D7N) and English (H6R) Familial Alzheimer Disease Mutations Accelerate Aβ Fibril Formation without Increasing Protofibril Formation. *J. Biol. Chem. 282*, 4916−4923.
(28) Viet, M. H., Nguyen, P. H., Derreumaux, P., and Li, M. S. (2014) Effect of the English Familial Disease Mutation (H6R) on the Monomers and Dimers of Aβ40 and Aβ42. *ACS Chem. Neurosci. 5*, 646−657.
(29) Girvan, P., Miyake, T., Teng, X., Branch, T., and Ying, L. (2016) Kinetics of the Interaction between Copper and Amyloid-β with FAD Mutations and Phosphorylation at the N-terminus. *ChemBioChem 17*, 1732−1737.
(30) Johnson, K. A., Simpson, Z. B., and Blom, T. (2009) Global kinetic explorer: a new computer program for dynamic simulation and fitting of kinetic data. *Anal. Biochem. 387*, 20−29.
(31) Boehr, D. D., Nussinov, R., and Wright, P. E. (2009) The role of dynamic conformational ensembles in biomolecular recognition. *Nat. Chem. Biol. 5*, 789−796.
(32) Rice, M. E. (2000) Ascorbate regulation and its neuroprotective role in the brain. *Trends Neurosci. 23* (5), 209−216.
(33) Hyslop, P. A., Zhang, Z., Pearson, D. V., and Phebus, L. A. (1995) Measurement of striatal H_2O_2 by microdialysis following global forebrain ischemia and reperfusion in the rat: correlation with the cytotoxic potential of H_2O_2 in vitro. *Brain Res. 671* (2), 181−186.
(34) Liu, D., Wen, J., Liu, J., and Li, L. (1999) The roles of free radicals in amyotrophic lateral sclerosis: reactive oxygen species and elevated oxidation of protein, DNA, and membrane phospholipids. *FASEB J. 13* (15), 2318−2328.

DOI: 10.1021/acs.biochem.8b00133
Biochemistry 2018, 57, 6228−6233